An extended difference of coherence test for comparing and combining several independent coherence estimates: theory and application to the study of motor units and physiological tremor

A.M. Amjad [a], D.M. Halliday [a,*], J.R. Rosenberg [a], B.A. Conway [b]

[a] *Division of Neuroscience and Biomedical Systems, Institute of Biomedical and Life Sciences, University of Glasgow, Glasgow G12 8QQ, UK*
[b] *Bioengineering Unit, University of Strathclyde, Glasgow G4 0NW, UK*

Abstract

Recently there has been an increase in the use of spectral methods for the analysis of experimental data. These analytical methods allow the study of interactions between simultaneously recorded signals and are particularly suited to the study of systems displaying rhythmic behaviour. A useful parameter in this context is the coherence function which provides a bounded measure of linear association between two signals. In this report we introduce two new techniques for dealing with an arbitrary number of independent coherence estimates. The first technique provides a test to compare the coherence estimates for statistically significant differences. The second allows the original coherence estimates to be combined, or 'pooled' into a single representative estimate. These two measures, taken together, provide a powerful tool for characterising and summarising the correlations within data sets. Applications of the techniques are illustrated by analysing the interactions between single motor unit discharges and finger tremor, and between pairs of motor unit discharges in human subjects. © 1997 Elsevier Science B.V.

Keywords: Coherence; Difference of coherence; Motor unit; Motor unit synchronization; Spectral analysis; Tremor

1. Introduction

In neurophysiology, correlation techniques have been widely used to investigate dependencies between signals, and to determine signal pathways in the central nervous system. These investigations have traditionally been done in the time domain using, for example, Post Stimulus Time Histogram (PSTH) studies and spike triggered averaging (STA) studies. Recently there has been an increase in the use of spectral methods (see Rosenberg et al., 1989; Farmer et al., 1993; Hamm and McCurdy, 1995). A spectral based approach can have advantages over a time domain approach since it ex-

tends the range of questions that can be asked about experimental data by allowing the study of interactions between more than two simultaneously recorded signals or processes (Rosenberg et al., 1989; Halliday et al., 1996). Spectral methods are also particularly well suited to the study of systems displaying rhythmic behaviour (e.g. Conway et al., 1995b). In many cases estimates of time domain parameters equivalent to those mentioned above can be arrived at via the frequency domain (Halliday et al., 1996). One clear advantage of frequency domain parameters is that confidence limits for parameter estimates can be easily constructed, the expressions are simple and the quantities are generally independent of the characteristics of the data (Brillinger, 1981, 1983; Rosenberg et al., 1989; Halliday et al., 1996). This follows from the fact that the large sample statistical properties of the finite Fourier trans-

---

* Corresponding author. Present address: West Medical Building, University of Glasgow, Glasgow G12 8QQ, UK. Tel.: +44 141 3304759; fax: +44 141 3304100; e-mail: gpaa34@udcf.gla.ac.uk

form of a stationary process are often simpler than those of the process itself, and lead to easily managed quantities suitable for the construction of confidence limits. (Brillinger, 1974, 1983).

A useful parameter for characterising the linear interaction between two processes in the frequency domain is the coherence function (Brillinger, 1981; Rosenberg et al., 1989; Halliday et al., 1996), estimates of which provide a bounded measure of linear association between two processes. The coherence function has two advantages over time domain measures of association. (1) It is a bounded measure, constrained within the range 0–1, with zero occurring in the case of independence, and one in the case of a perfect linear relationship. (2) It is a unitless measure, i.e. it does not depend on the units of measurement. In addition, the large sample properties of coherence estimates are known for the case of both dependent and independent processes (Brillinger, 1981; Rosenberg et al., 1989; Halliday et al., 1996). In the dependent case of two correlated processes a simple transformation, $(\mathrm{Tan}\,h^{-1})$, of the estimated coherence results in an expression with constant variance. This procedure has been used to construct a test to determine if two independent coherence estimates are statistically different (Brillinger, 1981; Rosenberg et al., 1989), and has been referred to as the 'difference of coherence' test.

While some progress has been made in determining the sampling distributions of time domain parameter estimates, the resulting expressions are generally complex in nature (Torres-Melo, 1974), rely on frequency domain parameters for their estimation (Rigas, 1983; Conway et al., 1993; Halliday et al., 1996), and are only valid under the assumptions of Poisson spike train data (Sears and Stagg, 1976), or a more general condition of independence (Brillinger et al., 1976; Rigas, 1983; Conway et al., 1993; Halliday et al., 1996). The implications of this last point are particularly important since most cases of interest will be when there is a dependence between signals. In practice this means that, as yet, no statistical test exists for comparison of two or more independent time domain parameter estimates. Some previous work on time domain correlation studies of spike train data has dealt with the derivation and application of synchronization indices, measures derived from cross correlation histograms. These measures are intended to provide an estimate of the strength of correlation between two spike trains. Given the above comments about sampling distributions of time domain measures, direct comparison of two or more of these synchronization indices may be misleading.

The aims of the present report are twofold. First to extend the difference of coherence test by introducing a measure which can be used to compare an arbitrary number of independent coherence estimates for statistically significant differences. Second to introduce the measure of 'pooled coherence' which combines several independent coherence estimates into a single estimate representative of all the data. These two measures, taken together, provide a powerful tool for characterising and summarising the correlations within data sets. The data sets could consist, for example, of a series of recordings of the same signals obtained from the same subject under different experimental conditions, allowing task dependency to be studied, or a series of recordings of different signals obtained from different subjects. Both these situations are illustrated in this report, the first by analysing the interactions between single motor unit discharges and finger tremor in human subjects with increased inertial loading, the second by comparing the coupling between different pairs of motor unit discharges obtained from different subjects. The key assumption of independent coherence estimates places no restrictions on the number of such estimates which can be included in an analysis. A preliminary account of this work has appeared in abstract form (Halliday et al., 1995).

2. Analytical methods

In the present report we will consider both time series and point process data. A time series is a real valued sequence, which we denote by $x(t)$, with sample values, denoted by x_t, available at equispaced intervals equal to the sampling interval. A point process, which we denote by N, may be defined as a random non-negative integer valued measure (Rosenberg et al., 1989), and in practice this leads to the ordered times of occurrence of discrete events (spikes) being the principle quantities available for analysis. The representation of neuronal spike trains by stochastic point processes is discussed in Conway et al. (1993). The tremor acceleration signal is treated as a time series, and motor unit spike trains as point processes.

The mathematical framework for the analysis is that of stationary interval processes, set out in Brillinger (1972) and Brillinger (1974). These processes can be used to represent either point process or time series data. Extensive development of this framework can be found, including estimation procedures and examples in Brillinger (1981) for time series data, in Rosenberg et al. (1989) for point process data, and in Halliday et al. (1996) for mixed (or hybrid) point-process/time-series data.

The processes are assumed to be second order stationary and satisfy a mixing condition, where values widely separated in time are independent. Time series are assumed to be zero mean, and point processes are assumed to be orderly, such that only one event occurs in a small interval dt (the sampling interval). These

assumptions are further discussed in Brillinger (1981), Rosenberg et al. (1989), Conway et al. (1993) and Halliday et al. (1996).

Before considering the finite Fourier transform of a point process it is necessary to introduce the notation for differential increments. For a point process, N, the counting variate $N(t)$ counts the number of events in the interval $(0,t]$. The differential increment, denoted by $dN(t)$, is defined as $dN(t) = N(t, t + dt]$. This counts the number of events in a small interval of duration dt starting at time t, and in practice since the process N is assumed to be orderly will take on the value 0 or 1 depending on the occurrence of a spike in the sampling interval dt.

The spectral estimation procedure used in the present report is the method of disjoint sections, as set out for point process data in Rosenberg et al. (1989) and Halliday et al. (1996) for hybrid data. Using this method, the complete record, denoted by R, is divided into L non-overlapping disjoint sections each of length T. The finite Fourier transform of the lth segment $(l = 1,..., L)$ from time series $x(t)$ at frequency λ is denoted by $d_x^T(\lambda, l)$, and defined as (Brillinger, 1972)

$$d_x^T(\lambda, l) = \int_{(l-1)T}^{lT} x(t)e^{-i\lambda t}dt \approx \sum_{t=(l-1)T}^{lT-1} e^{-i\lambda t}x_t \qquad (2.1)$$

For point process data the finite Fourier transform of a segment of length T from process N is denoted by $d_N^T(\lambda, l)$, and defined as (Brillinger, 1972; Rosenberg et al., 1989)

$$d_N^T(\lambda, l) = \int_{(l-1)T}^{lT} e^{-i\lambda t}dN(t) \approx \sum_{(l-1)T \le \tau_j < lT} e^{-i\lambda \tau_j} \qquad (2.2)$$

where τ_j are the times of occurrence of the N events.

In the following derivation we will denote the stationary interval processes to be considered by a, b. If the interval process a represents a time series, the finite Fourier transform of the lth segment, $d_a^T(\lambda, l)$, is given by Eq. (2.1), if process a is a point process then Eq. (2.2) is the appropriate equation. Similar comments apply to $d_b^T(\lambda, l)$. The distinction between point process and time series data will no longer be made, the following derivations are valid for all types of combinations of the two data types (Brillinger, 1983).

The cross spectrum between processes a and b is denoted by $f_{ab}(\lambda)$. A consistent estimate, denoted by $\hat{f}_{ab}(\lambda)$, and estimated using the method of disjoint sections, is given by (Brillinger (1981); Rosenberg et al. (1989); Halliday et al. (1996))

$$\hat{f}_{ab}(\lambda) = \frac{1}{2\pi LT}\sum_{l=1}^{L} d_a^T(\lambda, l)\overline{d_b^T(\lambda, l)} \qquad (2.3)$$

where the overbar '⏜' on $d_b^T(\lambda, l)$ indicates a complex conjugate. The auto spectrum of process a, denoted by $f_{aa}(\lambda)$, is estimated by replacing the subscript b with a in Eq. (2.3). A similar procedure applies for the auto spectrum of process b, $f_{bb}(\lambda)$.

Given two stationary interval processes, a and b, the coherence between these, denoted by $|R_{ab}(\lambda)|^2$, can be defined, suppressing the dependency on section number l, as

$$|R_{ab}(\lambda)|^2 = \lim_{T \to \infty}|\text{corr}\{d_a^T(\lambda), d_b^T(\lambda)\}|^2 \qquad (2.4)$$

with $d_a^T(\lambda)$ and $d_b^T(\lambda)$ defined by Eq. (2.1) for time series data, and by Eq. (2.2) for point process data. This function can be seen to be the magnitude squared of the correlation between the finite Fourier transforms of a and b. An alternative definition of the coherence function in terms of the second order spectra of processes a and b is given by

$$|R_{ab}(\lambda)|^2 = \frac{|f_{ab}(\lambda)|^2}{f_{aa}(\lambda)f_{bb}(\lambda)} \qquad (2.5)$$

Eq. (2.5) leads naturally to an estimation procedure by direct substitution of estimates of spectra, obtained from Eq. (2.3). The complex valued function representing the square root of Eq. (2.5) is called the coherency, following Wiener (1930). It is defined by

$$R_{ab}(\lambda) = \frac{f_{ab}(\lambda)}{\sqrt{f_{aa}(\lambda)f_{bb}(\lambda)}} \qquad (2.6)$$

Coherency functions are complex valued, and will have magnitude and phase components associated with them. An estimation procedure for Eq. (2.6) follows in a similar fashion to Eq. (2.5) by substitution of estimates of the spectra. Estimates of coherency functions are the starting point for the present analysis.

In the following discussion it is assumed we are considering k independent pairs of processes, where each pair is denoted by (a_i, b_i: $i = 1,..., k$). We denote the magnitude of the estimated coherency between the ith pair of processes, $|\hat{R}_{a_i b_i}(\lambda)|$, as $|\hat{R}_i|$. Applying Fisher's transform, $\text{Tan } h^{-1}$, the variance of the transformed estimated coherency is given by the constant value (Brillinger, 1981; Rosenberg et al., 1989)

$$\text{var}\{\text{Tan } h^{-1}|\hat{R}_i|\} = \frac{1}{2L_i} \qquad (2.7)$$

where L_i is the number of disjoint sections used to estimate the second order spectra for the ith pair of processes. The null hypothesis to be tested is that the k transformed coherency estimates have a common mean, and therefore the k original coherence estimates have a common mean. Denoting the Fisher transform, $\text{Tan } h^{-1}|\hat{R}_i|$, of the ith pair as $\hat{z}_i$, then an estimate of this common mean, denoted by $\bar{z}$, which has minimum variance, may be obtained by weighting the values $\hat{z}_i$ inversely as their variances

$$\bar{z} = \frac{\sum_{i=1}^{k} 2L_i\hat{z}_i}{\sum_{i=1}^{k} 2L_i} = \frac{\sum_{i=1}^{k} L_i\hat{z}_i}{\sum_{i=1}^{k} L_i} \qquad (2.8)$$

Then, under the above null hypothesis, the sum

$$\sum_{i=1}^{k} 2L_i(\hat{z}_i - \bar{z})^2 \tag{2.9}$$

is distributed approximately as χ^2 with $(k-1)$ degrees of freedom, where the mean $\bar{z}$ is computed from the data. The test statistic, Eq. (2.9), will contain a bias, this can be minimized by increasing the number of segments (ΣL_i). For the numbers of segments in the present results this bias will be negligible and can be ignored. The computation of this test statistic can be simplified to allow direct numerical calculation from the data by combining Eq. (2.8)) and Eq. (2.9) to give

$$2\left[\sum_{i=1}^{k} L_i\hat{z}_i^2 - \frac{\left(\sum_{i=1}^{k} L_i\hat{z}_i\right)^2}{\sum_{i=1}^{k} L_i}\right] \tag{2.10}$$

The computation of Eq. (2.10) is done separately at each frequency, λ, over the range of interest. A confidence limit at the $100(1-\alpha)\%$ level can be set at the value $\chi^2_{(\alpha;k-1)}$ and the null hypothesis rejected if the variate Eq. (2.10) exceeds this limit. Estimated values of Eq. (2.10) below this level would indicate that the null hypothesis of equal coherence estimates is plausible at that frequency, λ. The above test represents an extension of the difference of two independent coherence estimates, (see Section 1; Brillinger, 1981; Rosenberg et al., 1989) to deal with an arbitrary number of independent coherence estimates.

We may replace the original coherence estimates with a single coherence, which we call the pooled coherence estimate. This can be done by combining or 'pooling' the individual second order spectra using a weighting scheme similar to above and computing the pooled estimate of coherence in the manner of Eq. (2.5) as

$$\frac{\left|\sum_{i=1}^{k} \hat{f}_{a_ib_i}(\lambda)L_i\right|^2}{\left(\sum_{i=1}^{k} \hat{f}_{a_ia_i}(\lambda)L_i\right)\left(\sum_{i=1}^{k} \hat{f}_{b_ib_i}(\lambda)L_i\right)} \tag{2.11}$$

where $\hat{f}_{a_ib_i}(\lambda)$ denotes an estimate of the second order spectrum $f_{a_ib_i}(\lambda)$ estimated from L_i disjoint sections. Pooled coherence estimates, like ordinary coherence estimates, have values constrained within the range 0 to 1. The upper 95% confidence limit for an estimate of Eq. (2.11) based on the assumption of independence between the k pairs of processes is given by

$$1 - (0.05)^{1/(\Sigma L_i - 1)} \tag{2.12}$$

where ΣL_i is the total number of segments in the pooled coherence estimate. Values of the pooled estimate of coherence lying below this line can be taken as evidence that, on average, no coupling occurs between the two processes (a, b) at a particular frequency, λ. For the

individual coherence estimates, $|\hat{R}_{a_ib_i}(\lambda)|^2$, an upper 95% confidence limit, based on the assumption of independence, can be estimated by $1 - (0.05)^{1/(L_i-1)}$ (Brillinger, 1981; Rosenberg et al., 1989; Halliday et al., 1996)

If the data from the k pairs of processes supports the null hypothesis that the k transformed coherency estimates have a common mean, then we can interpret Eq. (2.11) as representative of each coherence estimate between the k pairs of processes. In situations where the coefficient Eq. (2.10) does not support the null hypothesis the pooled coherence estimate can still provide useful information about the processes under study, by providing a single summary coherence estimate.

The above analysis requires all second order spectra to be estimated with the same spectral bandwidth, i.e. with the same value of T. If the individual pooled spectra in Eq. (2.11) are used in an analysis then a further correction factor of $\left(\sum_{i=1}^{k} L_i\right)^{-1}$ is required for each of the three pooled spectral estimates in Eq. (2.11). For example, the inverse Fourier transform of the pooled cross spectrum can be used to compute an estimate of the pooled cumulant density function (see Halliday et al., 1996), providing a time domain measure of association between the k pairs of processes.

3. Results

The above techniques will be illustrated by their application to several data sets. These data sets are drawn from a data base of motor unit and tremor recordings made from normal healthy adult human subjects. Recordings were made with informed consent from each subject, and with local ethical committee approval. The tremor signal was derived from an ac-
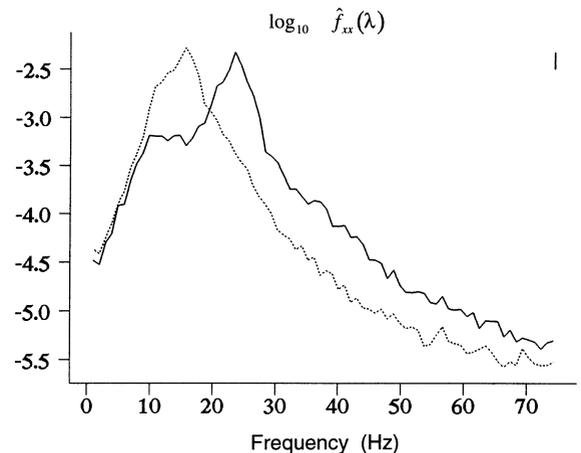
Fig. 1. Log plot of estimated auto spectrum of tremor signal, $\hat{f}_{xx}(\lambda)$ for data set one, with 0 g load (solid line) and 25 g load (dotted line). The solid vertical line at the top right shows the magnitude of the 95% confidence interval for the estimates (see Halliday et al., 1996).

A

$|\hat{R}_{xo}(\lambda)|^2$ 0 grammes

B

$|\hat{R}_{xo}(\lambda)|^2$ 5 grammes

C

$|\hat{R}_{xo}(\lambda)|^2$ 10 grammes

D

$|\hat{R}_{xo}(\lambda)|^2$ 15 grammes

E

$|\hat{R}_{xo}(\lambda)|^2$ 20 grammes

F

$|\hat{R}_{xo}(\lambda)|^2$ 25 grammes
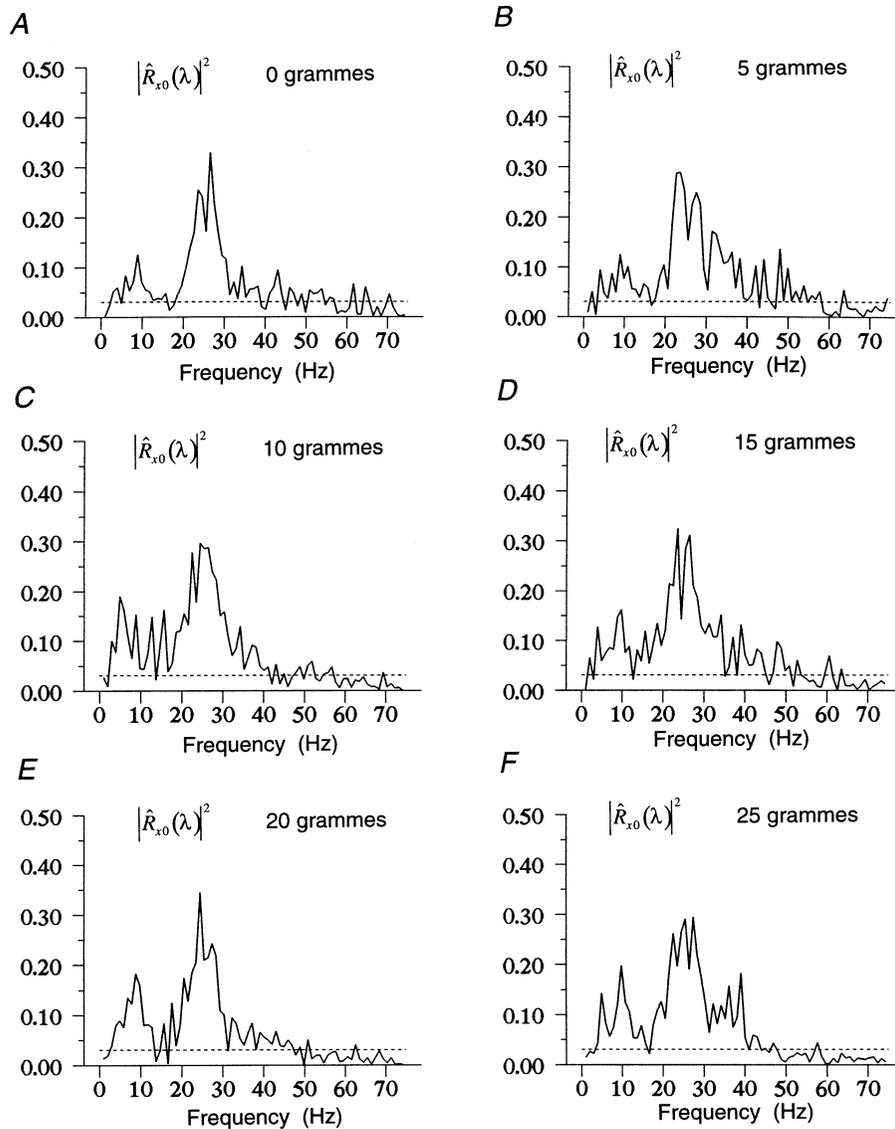
Fig. 2. Estimated coherences between a single motor unit discharge and tremor, $|\hat{R}_{xo}(\lambda)|^2$, for the six records in data set one, with added loads of (A) 0, (B) 5, (C) 10, (D) 15, (E) 20 and (F) 25 g. The horizontal dashed line in each graph represents an estimate of the upper 95% confidence limit based on the assumption of independence.

celerometer fixed to the distal phalanx of the unsupported middle finger maintained in an approximately horizontal position. The subject's other fingers, wrist and forearm were all supported by a custom designed rigid polypropylene cast. During data collection the subject was asked to extend and maintain the position of the unsupported middle finger. Pairs of single motor units were recorded from two concentric needle electrodes inserted into the extensor digitorum communis (EDC) muscle.

The accelerometer output (bandwidth DC — 200 Hz.) was amplified and fed to a data collection interface for digitising. The needle electrode signals were amplified and band pass filtered before being passed through window discrimination devices. The TTL

pulses output from these were fed to the digital input of the data collection device. Motor unit spike times were recorded to the nearest 1 ms, and the acceleration signal sampled at 1 ms intervals. Further details of the experimental protocol, as well as a description and detailed analysis of a single data set can be found in Halliday et al. (1996).

Physiological tremor is a complex signal resulting from interactions between several mechanical and neural factors (Elble and Koller, 1990). The spectrum of physiological tremor contains two types of components, which can be identified by distinct peaks in the estimated tremor spectrum. The dominant component is due in part to the mechanical resonance of the structure from which the tremor is recorded, and has been
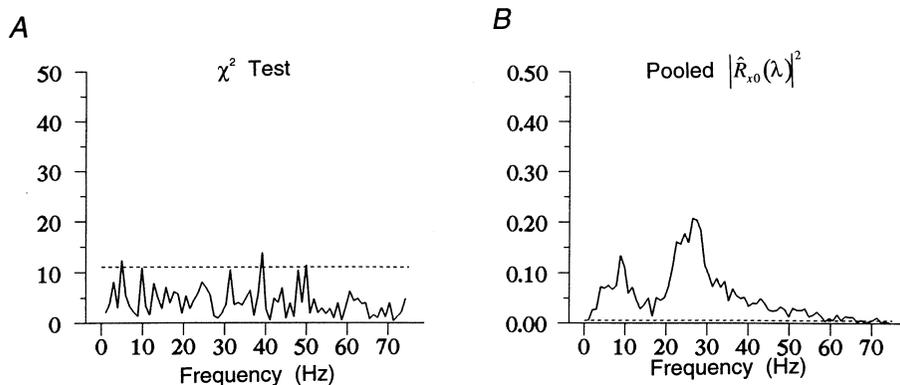
Fig. 3. (A) Computed values of χ^2 test statistic, Eq. (2.10), for the six records in data set one. Dashed line represents the upper 95% confidence limit under the null hypothesis of equal coherences. (B) Pooled estimate of coherence, Eq. (2.11), for the six records in data set one. Dashed line represents an estimate of the upper 95% confidence limit, Eq. (2.12), under the assumption of independent processes.

termed the mechanical reflex component of tremor (Stiles and Randall, 1967; Stiles, 1980). The frequency of this component of tremor can be altered by inertial loading. The other type of frequency components are load independent, and have been referred to as neurogenic components (Stiles and Randall, 1967; Elble and Koller, 1990). Neurogenic components have been shown to contribute to two distinct frequency bands of the tremor spectrum (Amjad et al., 1994). Increased inertial loading can be used to investigate which components in tremor spectra are mechanical reflex, and which are neurogenic (Stiles and Randall, 1967).

The above χ^2 test, Eq. (2.10), provides a framework to assess if coupling between tremor related signals is neurogenic, i.e. that coherence estimates are not affected by inertial loading. The first example examines the effect of increased inertial loading on motor unit-tremor coupling in a data set consisting of a series of six recordings from the same motor unit. The inertial loading is provided by the addition of weights to the
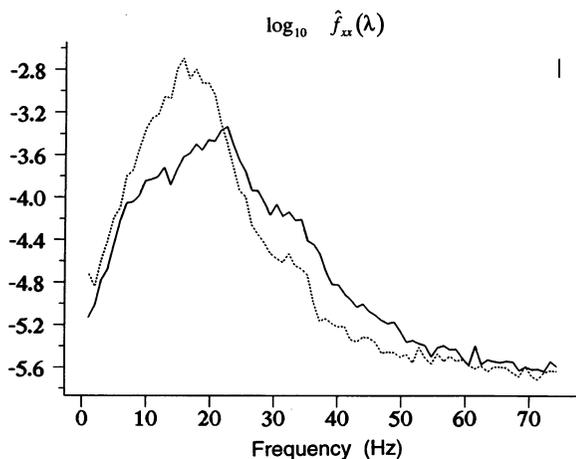
end of the unsupported finger, ranging from 0 to 25 g mass, in 5 g increments. The acceleration signal is assumed to be a realisation of stationary time series, which we denote by x. The sequence of motor unit firing times is assumed to be a realisation of a stationary and orderly point process, which we denote by N_0. Each record is 100 s in duration and was processed according to the methods set out above, where the record, R, was split into L complete disjoint sections each of length T ($T = 1024$, $R = 100\,000$ giving $L = 97$). After estimating auto spectra, cross spectra and coherency for all six records, the variate Eq. (2.10) and the pooled estimate of coherence, Eq. (2.11), were computed. For this data, $L_i = 97$; $i = 1, \ldots, 6$. The segment length of $T = 1024$, along with the sampling interval of 1 ms determines the spectral resolution, 0.97 Hz.

In Fig. 1 are shown autospectral estimates of the finger acceleration signal, $\hat{f}_{xx}(\lambda)$, estimated from Eq. (2.3), for the first and last record, corresponding to 0 g (solid line) and 25 g (dotted line) added mass. These are plotted on a log scale, the vertical bar on the right of the graph represents an estimate of the 95% confidence interval for the estimated spectra (Halliday et al., 1996), and provides a scale bar against which to assess the significance of distinct features in the spectra. The main difference between the two estimates is the downward shift of the dominant spectral peak from around 23 Hz with no loading to around 16 Hz with 25 g loading. This is the mechanical reflex component of tremor discussed above. Also present in the unloaded record is a component around 9–12 Hz, this is taken to be a neurogenic component which is masked in the other record by the dominant mechanical reflex component.

The coherence estimates between x and N_0, denoted by $|\hat{R}_{x0}(\lambda)|^2$ and estimated from Eq. (2.5), are shown in Fig. 2 for all six records in data set one, along with an estimate of the upper 95% confidence limits for these estimates (horizontal dashed lines). Despite the large downward shift in the dominant frequency of the

Fig. 4. Log plot of estimated auto spectrum of tremor signal, $\hat{f}_{xx}(\lambda)$ for data set two, with 0 g load (solid line) and 25 g load (dotted line). The solid vertical line at the top right shows the magnitude of the 95% confidence interval for the estimates.
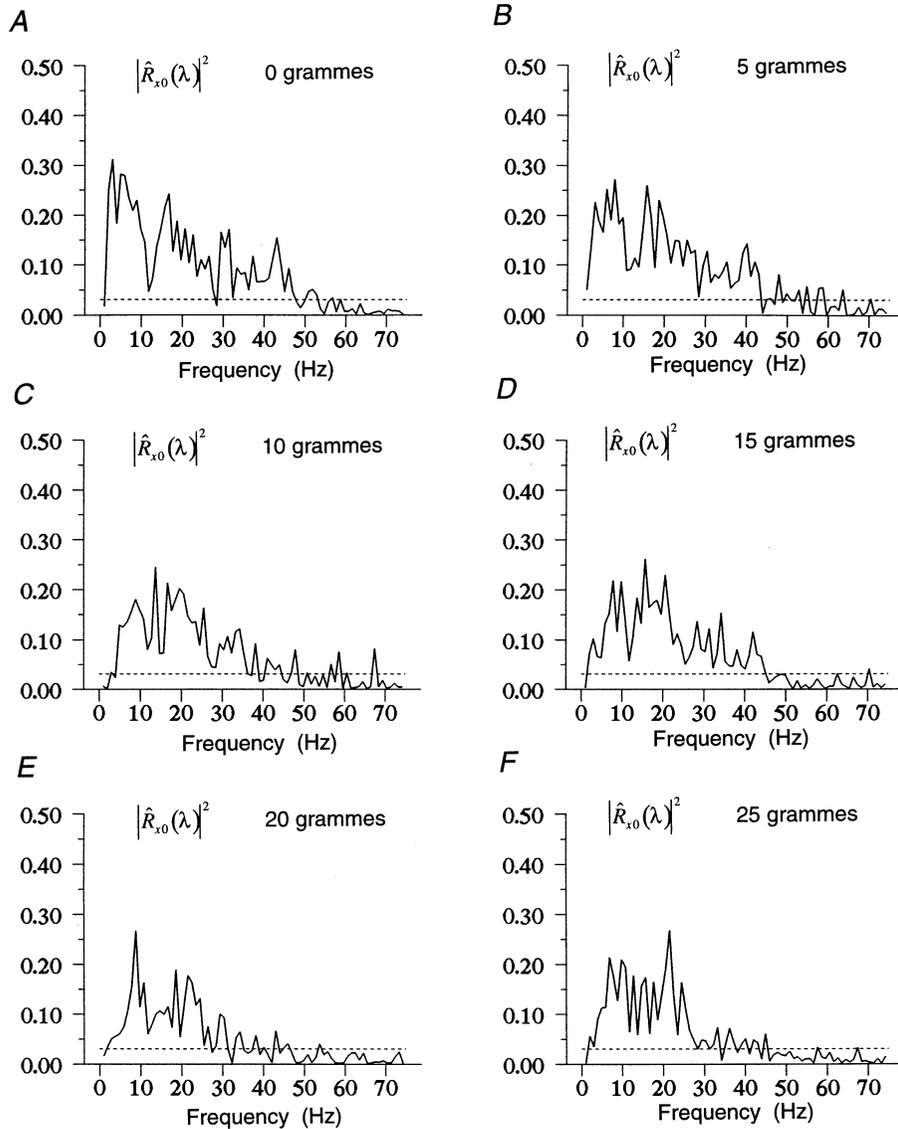
Fig. 5. Estimated coherences between a single motor unit discharge and tremor, $|\hat{R}_{x0}(\lambda)|^2$, for the six records in data set two, with added loads of (A) 0, (B) 5, (C) 10, (D) 15, (E) 20 and (F) 25 g. The horizontal dashed line in each graph represents an estimate of the upper 95% confidence limit based on the assumption of independence.

tremor spectrum, (Fig. 1), visual inspection of these coherence estimates indicates a similar range of significant coupling present in two distinct frequency bands, with a division around 15 Hz, a maximum around 10 Hz in the lower frequency band, and a maximum between 20–30 Hz in the higher frequency band. This is more clearly demonstrated by the results in Fig. 3. Fig. 3A shows the results of the χ^2 test, Eq. (2.10), along with the upper 95% confidence limit (dashed line, $\chi^2_{(0.05;5)} = 11.1$). Since almost all the values lie below the line, the null hypothesis of equal coherence estimates cannot be rejected for this data set. The pooled coherence estimate Eq. (2.11), along with the upper 95% confidence limit (Eq. (2.12), horizontal dashed line) are shown in Fig. 3B. It is clear from this figure that the

coherence is concentrated in two distinct frequency bands, with maxima at 9 Hz and 28 Hz. The minimum between the two frequency bands is located at 17 Hz. It is interesting to note that the mean firing rate of the motor unit ranged from 14.2 spikes/s at 0 g load to 16.3 spikes/s at 25 g load. This corresponds largely to the region where the pooled coherence in Fig. 3B is at a minimum. The significance of this result has been discussed elsewhere (Conway et al., 1995a). Elble and Randall (1976) found a similar result in coherence estimates between EDC motor units and tremor in force records. Their study, which involved much greater force levels and was restricted to frequencies below 25 Hz, found that coherence between motor units and tremor was generally not present at the firing rate of the
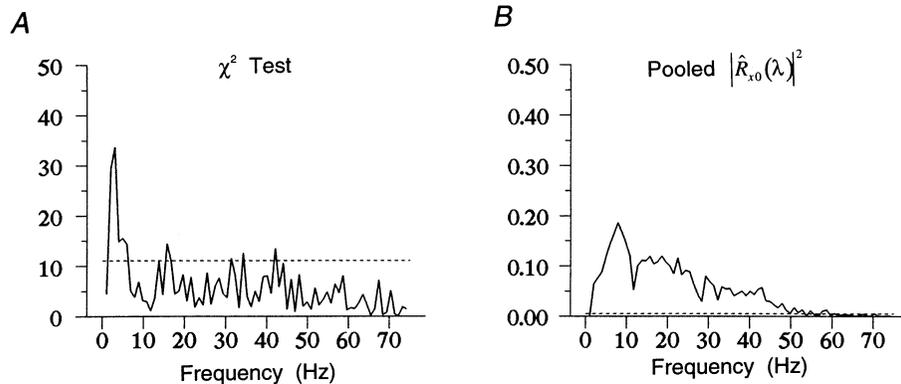
Fig. 6. (A) Computed values of χ^2 test statistic, Eq. (2.10), for the six records in data set two. Dashed line represents the upper 95% confidence limit under the null hypothesis of equal coherences. (B) Pooled estimate of coherence, Eq. (2.11), for the six records in data set two. Dashed line represents an estimate of the upper 95% confidence limit, Eq. (2.12), under the assumption of independent processes.

motor unit, but concentrated in the frequency band 8 to 12 Hz.

The second data set consists of the same series of measurements from a different subject. The results of the corresponding analysis for these six records are shown in Figs. 4–(6). The acceleration spectra in Fig. 4 are very similar to those in Fig. 1, with the dominant peak shifting down from around 23 Hz to around 16 Hz with increased inertial loading. In this example one neurogenic component can be seen for the unloaded case around 12 Hz, with a evidence of a second neurogenic component around 32 Hz. The six coherence estimates are shown in Fig. 5. There is a suggestion of banding in some of these coherence estimates, similar to that observed in data set one, but not as well defined in this case. The results of the χ^2 test are shown in Fig. 6A. This shows a significant difference in the coherence estimates over the range 2–6 Hz, with the maximum value of the χ^2 variate, Eq. (2.10), occurring at 3 Hz. The pooled coherence estimate in Fig. 6B no longer has the same interpretation as the one in Fig. 3B, however at frequencies higher than 6 Hz it can be considered as representative of the motor unit-tremor coupling over the six records. This estimate exhibits banding similar to that seen in Fig. 3B, with a distinct low frequency section centred around 9 Hz. The range of mean firing rate of the motor unit discharges in this case is from 10.9 spikes/s to 12.0 spikes/s, again corresponding to a minimum in the pooled coherence estimate.

The third example consists of 50 records of the discharges from motor unit pairs in EDC. Each record was obtained from a different motor unit pair, under the same experimental conditions as above, with the middle finger unloaded in all records. The data was collected during 20 experiments on 12 subjects. The record lengths vary from 20 to 180 s, with an average of 89 s. The range of firing rates is 7.5 spikes/s to 16.0 spikes/s, with an average of 11.7 spikes/s. The sequences of motor unit firing times are assumed to be

realisations of stationary and orderly point processes, denoted by N_0 and N_1. Before computing pooled parameter estimates, each motor unit pair underwent a process of 'temporal alignment', in which one spike train of the pair was adjusted by a constant time offset. This offset was chosen so that the peak in the time domain correlation between the spike trains was centred at zero lag, the offset was always an integer multiple of the sampling interval. The reason for this alignment is discussed below. Each pair was processed as above, $T = 1024$, with the range of values of L_i ($i = 1,\ldots, 50$) from 19 to 175. Estimates of the coherence function between N_0 and N_1, denoted by $|\hat{R}_{10}(\lambda)|^2$, and the cumulant density function, denoted by $\hat{q}_{10}(u)$, were constructed for each pair. Cumulant density functions provide a time domain measure of association between two processes, in the point process case they have an interpretation similar to a cross-correlation histogram. For further details, including estimation procedures and the construction of confidence limits for cumulant density function see Halliday et al. (1996).

Fig. 7 shows estimates of the coherence function, $|\hat{R}_{10}(\lambda)|^2$ and cumulant density function, $\hat{q}_{10}(u)$ for three examples from this data set. These examples all have the same record length of 100 s. The first example (Fig. 7A, B) has the strongest coupling, with significant coherence (Fig. 7B) in two distinct frequency bands around 0–10 Hz and 20–30 Hz. The corresponding cumulant density function (Fig. 7B) has a clear central peak illustrating the short term synchrony between the two motor unit discharges. The other two examples (Fig. 7C, D and Fig. 7E, F) show progressively weaker coupling between the motor unit discharges, indeed the last has barely any significant features in either the time or frequency domain estimates.

The pooled coherence, Eq. (2.11), and pooled cumulant density estimates are shown in Fig. 8A and B, respectively. The pooled cumulant density is estimated as the inverse Fourier transform of the pooled cross
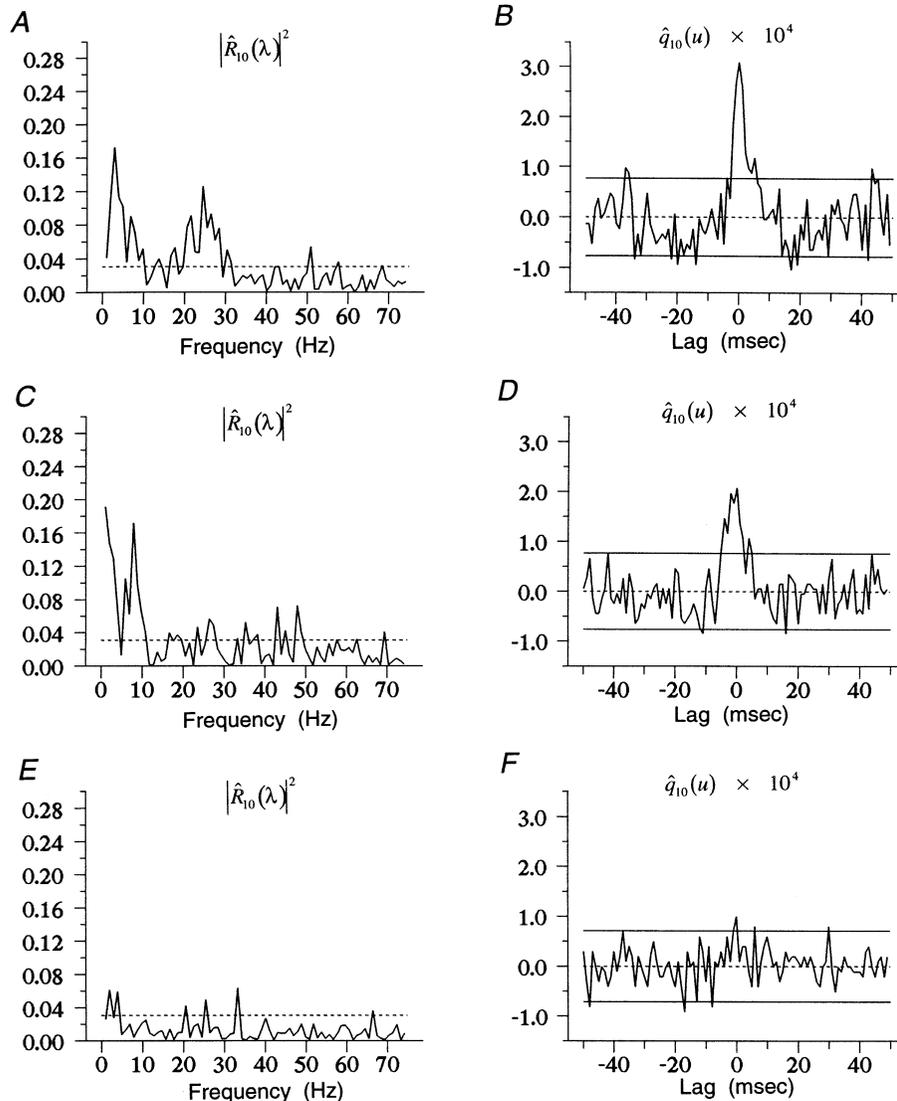
Fig. 7. (A, C, E) Estimated coherences between three pairs of motor unit discharges, $|\hat{R}_{10}(\lambda)|^2$. The horizontal dashed line in each graph represents an estimate of the upper 95% confidence limit based on the assumption of independence. (B, D, F) Estimated cumulant density between the same three pairs, $\hat{q}_{10}(u)$. The horizontal lines in each graph show the asymptotic value (dashed line at zero), and estimated upper and lower 95% confidence limits based on the assumption of independence (see Halliday et al., 1996).

spectrum, the confidence limits are estimated from the individual pooled auto spectra, according to the methods set out in Halliday et al. (1996). The pooled coherence illustrates the presence of two distinct frequency bands in the motor unit coupling, with the mean firing rate of 11.7 spikes/s corresponding to the minimum coherence between these two bands. In a similar study of motor unit coupling in human 1DI muscles, Farmer et al. (1993) observed significant coherence between pairs of motor units in the same two frequency bands. Fig. 8(a) confirms this finding for the EDC muscle. The technique used by Farmer et al. (1993) to detect weak coupling in a population was to construct a histogram of the percentage of estimates with a significant coherence estimate at each frequency. The present method

has the advantage of providing an estimate of the average strength of coupling within a population. In the present case the peak values of around 0.04 in the 0–10 Hz band and 0.015 in the 20–30 Hz band show we are dealing with weak correlations.

The pooled cumulant density estimate has a well defined time course, with a central peak of around 14 ms in width. The temporal alignment process described above was necessary since the peak in the individual cumulant density estimate was not always at zero lag. Computing the pooled cumulant density from the 50 motor unit pairs without this alignment resulted in a pooled cumulant density estimate with a much reduced peak spread over a broad range of lags compared to Fig. 8B. The difference in peak latencies for individual
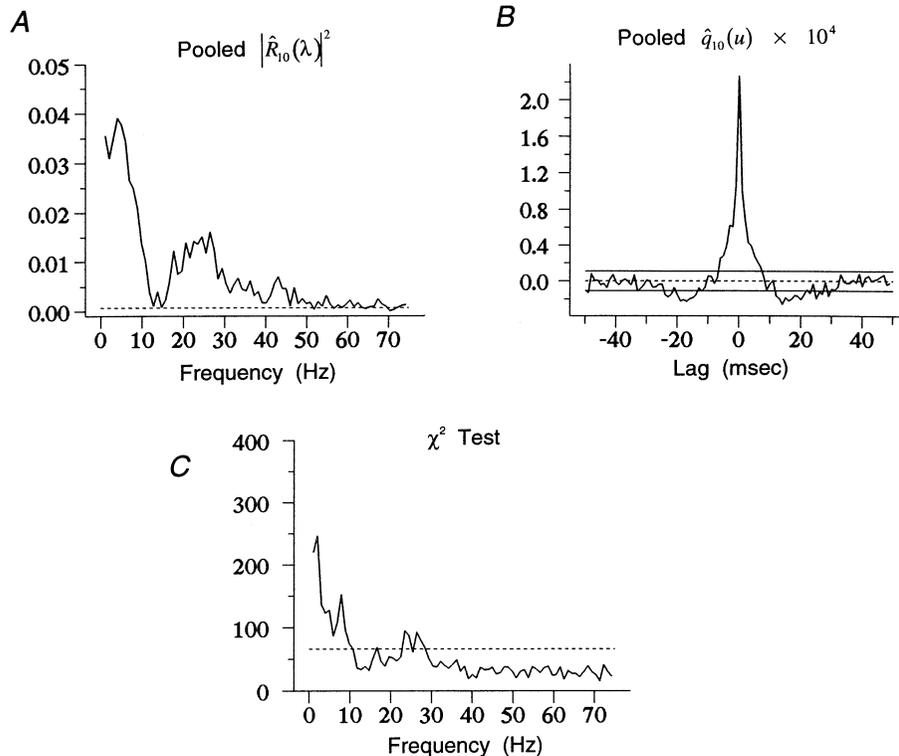
Fig. 8. (A) Pooled estimate of coherence, Eq. (2.11), for the 50 records from different motor unit pairs in data set three. Dashed line represents an estimate of the upper 95% confidence limit, Eq. (2.12), under the assumption of independent processes. (B) Pooled estimate of cumulant density for the same 50 pairs. The horizontal lines show the asymptotic value (dashed line at zero), and estimated upper and lower 95% confidence limits based on the assumption of independence. (C) Computed values of χ^2 test statistic, Eq. (2.10), for the 50 records in data set three. Dashed line represents the upper 95% confidence limit under the null hypothesis of equal coherences.

records is taken to reflect conduction delays in nerve and muscle, which the alignment process corrects for.

The individual examples in Fig. 7 indicate a wide variability in the estimated strength of coupling between individual motor unit pairs. This is borne out by the χ^2 test shown in Fig. 8C, plotted with the estimated upper 95% confidence limit (dashed line, $\chi^2_{(0.05;49)} = 66.3$). This shows that the hypothesis of equal coherences is rejected in the range 0–10 Hz and 22–28 Hz. This alters the interpretation of the pooled coherence in Fig. 8A, which cannot now be considered as representative of all the 50 individual coherence estimates. However, it does provide a single coherence estimate summarizing the coupling within the 50 motor unit pairs, illustrating that this coupling in the population is concentrated in two frequency bands, with a minimum at the mean firing rate. The three estimates in Fig. 7 will all have equal weight in this pooled coherence, since they all have the same value of L_i (97 segments).

4. Conclusions

In the present report a method has been introduced for comparing several coherence estimates from independent experiments, and combining the individual esti-

mates into a single pooled coherence estimate. These procedures represent an extension to spectral methods of techniques for comparison of correlation coefficients for random variables derived from large samples, (e.g., see Rao, 1973, chpt. 6). This approach complements the extensive framework set out in Halliday et al. (1996) for dealing with dependent processes. If the object of an analysis is to summarise the correlations within a data set, the methods presented in the present report may be preferable to the more traditional approach of using one 'illustrative' example, since they can include all the data, appropriately weighted.

The first two examples (Figs. 1–6) illustrate how these techniques can be used to investigate neurogenic features in coupling between tremor related signals. It is worth noting that the individual records of 100 s duration, which equate to data sets of 10^5 points, represent statistically 'large' sample sizes. Despite this it is not clear from visual inspection alone that the six coherences in Fig. 2 satisfy the hypothesis of equal coherence estimates, whereas those in Fig. 5 do not. In these two examples where the record lengths in each data set are equal, the pooled spectra in Eq. (2.11) are the average of the individual spectral estimates. The concept of averaging coherence estimates has been used previously in a neurophysiological context (Brillinger, 1992). Other

applications of these techniques include the study of task dependency in neural correlations.

The third example (Figs. 7 and 8) illustrates a slightly different approach to using these tools, namely the investigation of population effects in the coupling between processes, where it is required to summarise the coherence by estimating a weighted average. This is particularly useful where the coupling is weak with considerable variability between coherence estimates, as in the present case. Indeed, given the variability in the individual examples in Fig. 7, it would be unreasonable to expect that the null hypothesis of equal coherence estimates is verified, as is illustrated in Fig. 8C. Nonetheless, the pooled coherence estimate provides new insight into the strength of coupling within a large population of motor units recorded under the same experimental conditions, by providing a single measure which summarizes the coupling within this population. Computation of the pooled coherence estimate from weighted spectra, Eq. (2.11), means that pooled phase and cumulant density estimates (Fig. 8B) can be constructed, allowing population behaviour to be investigated in both time and frequency domains. This example is estimated from data equivalent to a single record of 73.3 min duration ($\Sigma L_i = 4296$), this results in pooled parameter estimates with greatly reduced standard errors, allowing weak correlations to be specified to a greater precision.

The above analysis would also be suitable for comparing several independent pooled estimates of coherences, as well as pooled estimates of partial coherences. Partial coherence estimates constructed using the method of disjoint sections (Halliday et al., 1996) have the same asymptotic distribution as ordinary coherence estimates, for all orders (Brillinger, 1981; Halliday et al., 1996). Thus expression Eq. (2.7) and the following derivation is valid for partial coherence estimates also. Estimation of the pooled partial coherence is achieved by substitution of the appropriate weighted partial spectra into an equation similar to Eq. (2.11).

Acknowledgements

References

Amjad, A.M., Conway, B.A., Farmer, S.F., Halliday, D.M., O'Leary, C. and Rosenberg, J.R. (1994) A load independent 30–40 Hz component of physiological tremor, J. Physiol., 476: 21P.

Brillinger, D.R. (1972) The spectral analysis of stationary interval functions. In LeCam, L.M., Neyman, I. and Scott, E. (Eds.), Proc. Sixth Berkeley Symp. Math. Stat. Prob., pp. 483–513.

Brillinger, D.R. (1974) Fourier analysis of stationary processes, Proc. IEEE, 62: 1628–1643.

Brillinger, D.R. (1981) Time Series-Data Analysis and Theory, 2nd edn, Holden Day, San Francisco.

Brillinger, D.R. (1983) The finite Fourier transform of a stationary process. In Brillinger, D.R. and Krishnaiah, P.R. (Eds.), Handbook of Statistics, Elsevier, Amsterdam, pp. 21–37.

Brillinger, D.R. (1992) Examples of scientific problems and data analyses in demography, neurophysiology, and seismology, J. Comput. Graph. Stat., 3: 1–22.

Brillinger, D.R., Bryant, H.L. and Segundo, J.P. (1976) Identification of synaptic interactions, Biol. Cybern., 22: 213–228.

Conway, B.A., Halliday, D.M. and Rosenberg, J.R. (1993) Detection of weak synaptic interactions between single Ia-afferents and motor-unit spike trains in the decerebrate cat, J. Physiol., 471: 379–409.

Conway, B.A., Farmer, S.F., Halliday, D.M. and Rosenberg, J.R. (1995a) On the relation between motor-unit discharges and physiological tremor. In Taylor, A., Gladden, M.H. and Durbaba, R (Eds.), Alpha and Gamma Motor Systems, Plenum Press, New York, pp. 596–598.

Conway, B.A., Halliday, D.M., Farmer, S.F., Shahani, U., Maas, P., Weir, A.I. and Rosenberg, J.R. (1995b) Synchronization between motor cortex and spinal motoneuronal pool during the performance of a maintained motor task in man, J. Physiol., 489: 917–924.

Elble, R.J. and Koller, J. (1990) Tremor, John Hopkins, Baltimore.

Elble, R.J. and Randall, J.E. (1976) Motor unit activity responsible for 8- to 12-Hz component of human physiological tremor, J. Neurophysiol., 39: 370–383.

Farmer, S.F., Bremner, F.D., Halliday, D.M., Rosenberg, J.R. and Stephens, J.A. (1993) The frequency content of common synaptic inputs to motoneurones studied during voluntary isometric contraction in man, J. Physiol., 470: 127–155.

Halliday, D.M., Amjad, A.M., Conway, B.A., Farmer, S.F. and Rosenberg, J.R. (1995) A method for comparison of several coherence estimates from independent experiments, J. Physiol., 487: 76P.

Halliday, D.M., Rosenberg J.R., Amjad, A.M., Breeze, P., Conway, B.A. and Farmer, S.F. (1996) A framework for the analysis of mixed time series/point process data: theory and application to the study of physiological tremor, single motor unit discharges and electromyograms, Prog. Biophys. Mol. Biol., 64: 237–278.

Hamm, T.M. and McCurdy, M.L. (1995) The use of coherence spectra to determine common synaptic inputs to motoneurone pools of the cat during fictive locomotion. In Taylor, A., Gladden, M.H. and Durbaba, R (Eds.), Alpha and Gamma Motor Systems, Plenum Press, New York, pp. 309–315.

Rao, C.R. (1973) Linear Statistical Inference and its Applications, 2nd edn, Wiley, New York.

Rigas, A. (1983) Point process and time series analysis: Theory and applications to complex physiological systems. Ph.D. Thesis, Glasgow University.

Rosenberg, J.R., Amjad, A.M., Breeze, P., Brillinger, D.R. and Halliday, D.M. (1989) The Fourier approach to the identification of functional coupling between neuronal spike trains, Prog. Biophys. Mol. Biol., 53: 1–31.

Sears, T.A. and Stagg, D. (1976) Short-term synchronization of intercostal motoneurone activity, J. Physiol., 263: 357–387.

Stiles, R.N. (1980) Mechanical and neural feedback factors in postural hand tremor of normal subjects, J. Neurophysiol., 44: 40–59.

Stiles, R.N. and Randall, J.E. (1967) Mechanical factors in human tremor frequency, J. Appl. Physiol., 23: 324–330.

Torres-Melo, L. (1974) Stationary Point Processes. Ph.D. Thesis, University of California, Berkeley.

Wiener, N. (1930) Generalized harmonic analysis. Acta. Math., 55: 117–258.